Gravity experiments in strong fields using pulsars as clocks

H. Hu, M. Kramer, N. Wex, D. J. Champion

Max-Planck-Institut für Radioastronomie

Abstract

Pulsars are precise cosmic clocks, some of which can rival the stability of the best atomic clocks on long timescales. In addition, pulsars are strongly self-gravitating bodies, and pulsars in binary systems provide excellent testbeds for gravity experiments in the strong-field regime. Timing the pulses from pulsar itself enables precise measurements of a wide range of relativistic effects, such as orbital precession, time dilation, Shapiro delay, and orbital period decay due to gravitational wave damping. In particular, the Double Pulsar system PSR J0737-3039A/B enables measurements of these effects with unprecedented precision, all of which general relativity (GR) has passed with flying colors. Based on 3-yr MeerKAT observations of PSR J0737-3039A, we further investigate the next-to-leading-order (NLO) signal propagation effects, including the retardation effect due to the movement of pulsar B and the deflection of the signal of pulsar A by the gravitational field of pulsar B. In addition, future observations with MeerKAT and the Square Kilometre Array (SKA) promise to provide one of the first measurements of the moment of inertia of a neutron star, hence an important complementary constraint on the equation of state of dense matter. Finally, other prospects for future observations of the Double Pulsar are also demonstrated, such as potential measurements of lensing, moment of inertia (and consequently equation of state of dense matter), frame-dragging, and NLO gravitational wave damping.

Gravity experiments with pulsars

Strong-field gravity experiments were enabled by the discovery of the first binary pulsar – PSR B1913+16 by Russell Hulse and Joseph Taylor in 1974 [1]. **By recording the arrival time of pulses over a period of time, a number of relativistic effects can be measured as "post-Keplerian"(PK) parameters.** Three such parameters were first measured in the first binary pulsar B1913+16 — **advance of periastron $\dot{\omega}$**, time dilation $\gamma_{\rm E}$ (gravitational redshift and second-order Doppler effect), and **orbital period decay $\dot{P}_{\rm b}$ due to gravitational wave (GW) damping** [2]. This provided the first evidence for the existence of GWs. Currently the most precise test of GR's quadrupolar description (2.5PN in the equations of motion) of GWs comes from a 16-yr timing analysis on the Double Pulsar, PSR J0737-3039A/B [3]. This unique system was discovered in 2003 [4,5], consisting of a old recycled pulsar (A, P=23 ms) and a young pulsar (B, P=2.8 s) in a mildly eccentric (e=0.088), 2.45-h orbit. Its highly inclined angle (i=89.35° or 90.65°) allows for additional relativistic test of the **Shapiro delay ("shape" *s* and "range" *r*) and its higher-order effects** [3]. Together with relativistic spin precession of pulsar B $\Omega_B^{\rm spin}$[6] and relativistic orbital deformation δ_θ, a total of seven PK parameters have been measured [3]. In addition, a mass ratio *R* can be determined from the sizes of the orbits of two pulsars. These eight parameters provide tight constraints on the two pulsar masses and six independent tests for theories of gravity. An example for testing GR is summarised in Fig. 2.

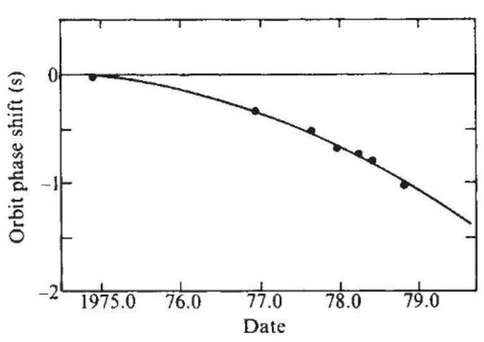

Fig. 1 Orbital decay in the binary pulsar B1913+16 demonstrated as shifts in periastron passage time. The parabola indicates GR's prediction for GW emission [2].

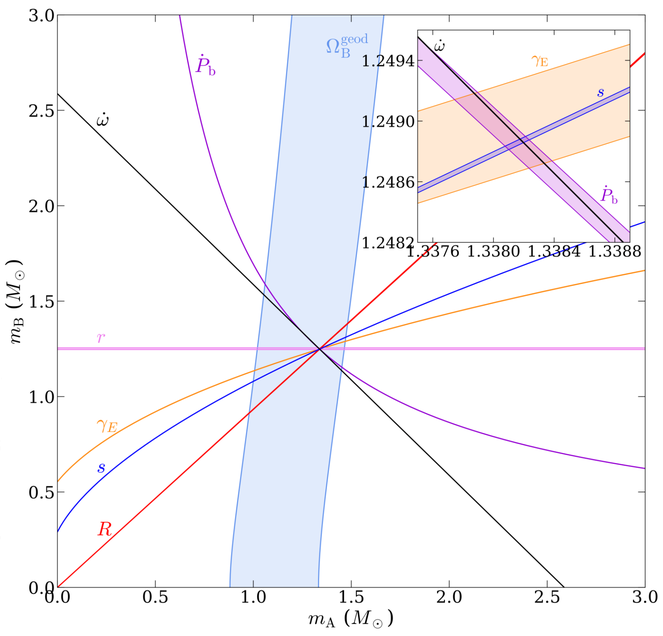

Fig. 2 (right) Mass-mass diagram for the Double Pulsar. Each pair of lines represents a measured PK parameters interpreted in GR [3].

Testing higher-order signal propagation effects

The Double Pulsar probes the strongest spacetime curvature among current gravity experiments that test photon propagation (including Event Horizon Telescope) [12]. MeerKAT observations on **PSR J0737-3039A** provide extraordinary timing precision, **allowing a quick improvement** on the measurements of **Shapiro delay and next-to-leading order (NLO) signal propagation effects** [13], including the retardation effect due to the movement of pulsar B and the deflection of the signal of pulsar A by the gravitational field of pulsar B. An example of the eclipse observation with MeerKAT is shown in Fig. 4, where the intensity modulation is caused by the eclipse of the plasma-filled magnetosphere of pulsar B. With **3-yr MeerKAT data**, the common factor for NLO signal propagation effects ($q_{\rm NLO}$ =1 in GR), including retardation, longitudinal deflection and lensing, is measured as $q_{\rm NLO}$=0.999(79), **giving a independent confirmation of these effects and improved by 1.65 times compared to the 16-yr result** [3]. The signal deflection not only causes a longitudinal time shift, but can also change the co-latitude of the emission direction towards Earth (see Fig. 6 and [13]). We found the **lensing** correction to Shapiro delay is difficult to observe separately as it is mostly absorbed by Shapiro parameter *s*, but with the precision of the full SKA, it can potentially be measured within a few years.

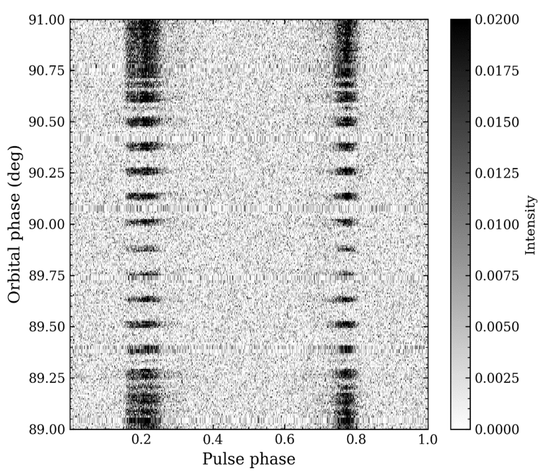

Fig. 4 MeerKAT eclipse data on PSR J0737-3039A.

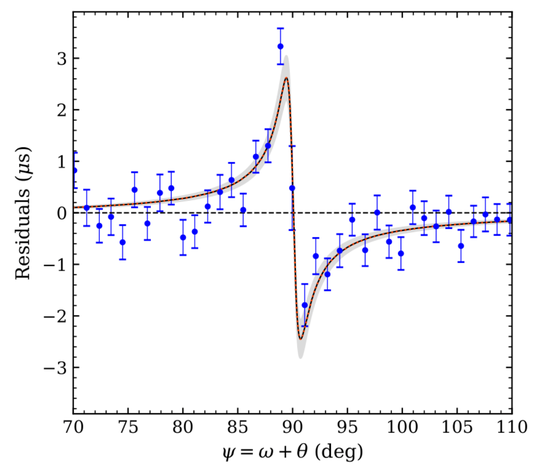

Fig. 5 Residuals showing the combination of retardation effect and longitudinal deflection delay [13].

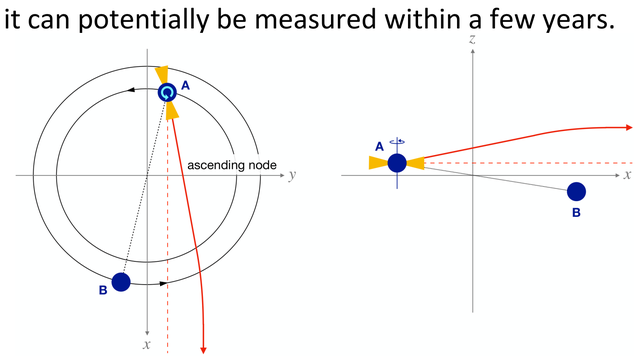

Fig. 6 (left) Illustration of the deflection effect of A's signal in the gravitational field of B, in the direction of longitude (left) and latitude (right) [13].

Moment-of-inertia of a neutron star

Mass measurements from radio pulsars have placed important constraints on the equation of state (EOS) of matter at supranuclear densities (Fig. 3). The moment of inertia (MOI) of a neutron star, on the other hand, directly encoding the relationship between mass and radius, can potentially identify the EOS even with a low-precision measurement [8]. For the Double Pulsar, the MOI of A ($I_{\rm A}$) will become measurable as a contribution to the observed periastron advance due to relativistic spin-orbit coupling (Lense-Thirring effect). **With MeerKAT and the SKA, a measurement with ~10% accuracy is possible by 2030** [9].

Fig. 3 Mass-radius relation for different EOSs. The horizontal bands indicate the 1-σ mass ranges for the two heaviest pulsars known. The light blue bar corresponds to the 90% confidence limit range of radii for 1.4 $M_\odot$ neutron stars [7].

Testing Lense-Thirring effect

If the EOS is known sufficiently well, one could in turn test the Lense-Thirring (LT) contribution to the periastron advance in a general form and constrain theories of gravity. It can be written as [10]

$$\dot{\omega}^{\rm LT,A} = -\frac{2n_{\rm b}^2 I_{\rm A}\Omega_{\rm A}}{\left(1-e_{\rm T}^2\right)^{3/2} M}\frac{\sigma_{\rm A}}{\mathcal{G}},$$

where $\sigma_{\rm A}$ is a generic strong-field spin-orbit coupling constant, and $\mathcal{G}$ the effective gravitational constant ($n_{\rm b}$-orbital frequency, $\Omega_{\rm A}$-angular spin frequency, $e_{\rm T}$-time eccentricity, M-total mass). **We found a 7% test of LT precession is possible by 2030** [9].

NLO gravitational wave damping

In the near future, our data will start to be sensitive to the NLO (3.5PN) GW damping, and **a 3σ-measurement can be expected by 2030.** The right side shows the expression of orbital period decay due to GW damping extended to 3.5PN in the equations of motion [11] (see [9] for details).

$$\begin{aligned}\dot{P}_{\rm b}^{\rm GR} = &-\frac{192\pi}{5}\frac{\eta\beta_{\rm O}^5}{(1-e_{\rm T}^2)^{7/2}}\left\{1+\frac{73}{24}e_{\rm T}^2+\frac{37}{96}e_{\rm T}^4\right.\\ &+\frac{\beta_{\rm O}^2}{336\,(1-e_{\rm T}^2)}\left[1273+\frac{16495}{2}e_{\rm T}^2+\frac{42231}{8}e_{\rm T}^4+\frac{3947}{16}e_{\rm T}^6\right.\\ &-\left(924+3381e_{\rm T}^2+\frac{1659}{4}e_{\rm T}^4-\frac{259}{4}e_{\rm T}^6\right)\eta\\ &\left.\left.+\left(3297e_{\rm T}^2+4221e_{\rm T}^4+\frac{2331}{8}e_{\rm T}^6\right)\frac{\delta m}{M}\right]\right\}\end{aligned}$$

Other applications of pulsars

Testing alternative theories of gravity

Pulsars also provide constraints on alternative theories of gravity, as dipolar GWs may exist in such theories and could be a leading contribution of GW damping. Fig.7 summarises constraints on Damour–Esposito-Farèse (DEF) gravity [14] from various pulsar experiments. Despite relatively low asymmetry in their compactness, the Double Pulsar still contributes important constraints for $\beta_0 \lesssim -3$ (red solid line) [3]. With MeerKAT and the SKA, we expect an even better constraint in the near future (red dashed line) [9].

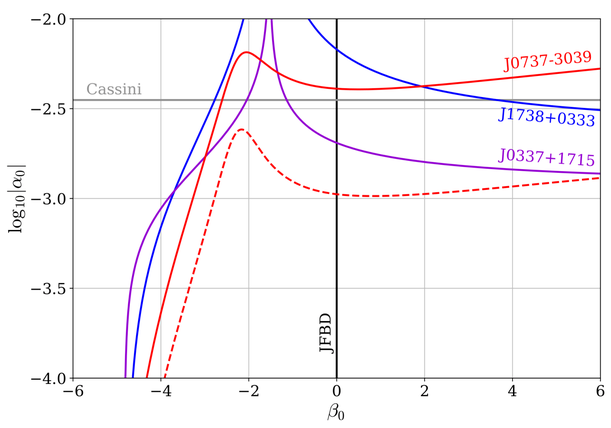

Fig. 7 Constraints on the DEF gravity from different pulsar experiments (see [3][9] for details). A stiff EOS MPA1 is assumed. Areas above a curve are excluded.

Searching for nanohertz GW using a pulsar timing array (PTA)

A network of stably rotating pulsars can served as a Galaxy-scale GW detector, namely the pulsar timing array (PTA). PTA is sensitive to GWs at nanohertz regime, primarily from inspiraling supermassive blackhole binaries at the centre of galaxies. The superposition of these binaries forms a GW background (GWB). Recently a common red signal has been detected in different PTA datasets, with spectral properties compatible with theoretical GWB predictions (see [15]).

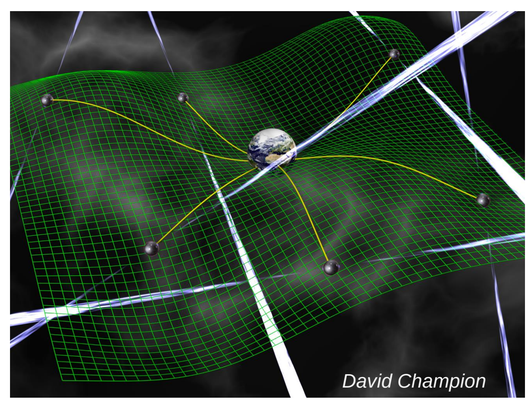

Fig. 8 Artistic illustration of a pulsar timing array.

References

[1] Hulse and Taylor, 1974, ApJL, 191, L59
[2] Taylor, Fowler & McCulloch, 1979, Nature, 277, 437
[3] Kramer et al., 2021, PRX 11, 041050
[4] Burgay et al., 2003, Nature, 426, 531
[5] Lyne et al., 2004, Science, 303, 1153
[6] Breton et al., 2008, Science, 321, pp.104
[7] Dietrich et al., 2020, Science, 370, pp. 1450-1453
[8] Lattimer & Schutz, 2005, ApJ, 629:979
[9] Hu et al., 2020, MNRAS, 497, 3, pp.3118-3130
[10] Damour & Taylor, 1992, PRD, 45, 1840
[11] Blanchet & Schäfer, 1989, MNRAS, 239, 845
[12] Wex & Kramer, 2020, Universe, 6(9), p. 156
[13] Hu et al., 2022, A&A, 667, A149
[14] Damour & Esposito-Farèse, 1993, PRL, 70, 2220
[15] Chen et al., 2022, MNRAS, 510, 4873